

Epoxycyclopentane Hydrate for Hydrate-Based Energy Storage: Notable Improvements in Thermodynamic Condition and Storage Capacity

Jiwoong Seol^{1*}, Juwoon Park² and Woongchul Shin³

¹ Faculty of Liberal Education, Seoul National University, 1 Gwanak-ro, Gwanak-gu, Seoul 08826, Republic of Korea

² Naval & Energy System R&D Institute, Daewoo Shipbuilding & Marine Engineering Co., LTD., Gyeonggi-do 15011, Republic of Korea

³ Central Technology R&D Institute, Hyundai Oilbank Co., LTD., Gyeonggi-do 16891, Republic of Korea

*corresponding author: seoljiwoong@snu.ac.kr

Table of Contents

1. Experimental methods	p. 2
2. Figures and additional descriptions	
(1) Figure S1	p. 4
(2) Figure S2	p. 5
(3) Figure S3	p. 6
(4) Figure S4	p. 7
(5) description for Figure 3(b)	p. 9
3. Tables S1~S4	p. 10
4. References (additional)	p. 11

1. Experimental methods

H₂O (LC-MS grade, Merck) and ECP (97%, Alfa Aesar) were used as received. High-purity CH₄ (99.95%) and H₂ (99.9%) were supplied by Daesung Industrial Gas Corp. of Korea. Compared to the stoichiometric composition ($x_{\text{ECP}} = 0.0556$), a slightly excessive (~5%) amount of ECP was mixed with water. The mixture was then charged in a high-pressure resistance cell (V~100ml) and pressurized with 65 bar of CH₄ or 90 bar of H₂ at room temperature. The cell in each case was gradually cooled from 303 K at a rate of -1 K•h⁻¹ with stirring maintained at 200 ± 10 RPM. The reactor was cooled to a sufficiently low temperature of approximately 263 K to obtain a sample in a fully converted state. The solid sample was quickly collected and immersed in liquid nitrogen. Finally, it was ground into a fine powder (d < 200 μm) for the subsequent spectroscopic analyses.

Synchrotron high-resolution powder diffraction (HRPD) patterns were measured with the beam-line 9B at the Pohang Accelerator Laboratory. Each pattern was obtained in a 2θ range of 5.0 to 126.0° (step width = 0.01° and scan time = 0.7 s/scan) using a single wavelength of 1.5216 Å. At the measurement temperature of 150 K, no dissociation of the hydrate samples was detected. The measured points (red dot) were then matched with whole-profile calculations using the FullProf program. The resulting functions (black curve) and χ values are presented in Figure 2.

Solid-state NMR experiments were conducted with the Bruker 400 MHz Avance II solid-state NMR at the Korea Basic Science Institute. For the ¹³C MAS NMR analysis (hpdec), we used a Larmor frequency of 100.4 MHz, a pulse length (p1) of 1.6 μs, and a repetition delay time (d1) of 3 s. For the ¹H MAS NMR analysis (one pulse), a radio frequency of 400 MHz, a pulse length (p1) of 1.5 μs, and a repetition delay time (d1) of 5 s were used. The static ¹³C and ¹H signals of tetramethylsilane were referred to as 0 ppm at room temperature. All

samples were measured at 210 K with a magic-angle spinning rate of 5 kHz.

The vibration frequencies of the guest molecules were studied with high-resolution Raman equipment (Horiba Jobin Yvon LabRam HR Evolution). A 532-nm laser at 50 mW was used as an excitation source. All Raman spectra were obtained at 123 K with a low-temperature Linkam accessory.

To estimate the promotion performance of ECP, the equilibrium P-T conditions were measured for the ECP + CH₄ and ECP + H₂ hydrate systems. Each liquid mixture (~ 7 g) with a stoichiometric composition ($x_{\text{ECP}} = 0.0556$) was charged into a high-pressure resistance cell (V ~100 ml) and pressurized at various CH₄ or H₂ pressures at room temperature. The samples were continuously cooled to 263 K (at a rate of -1 K•h⁻¹) to form a solid hydrate phase. They were then more slowly re-heated to 310 K (at a rate of 0.3 K•h⁻¹). The stirring speed was kept at 200 ± 10 RPM during the overall hysteresis process. To verify the accuracy of our measurements, several equilibrium points of the THF + CH₄ system were also measured. We note that our additional measurements of the THF + CH₄ hydrate (black empty diamond in Figure 4), as carried out to verify the accuracy of our experiment, demonstrated very good agreement with the reported values (black filled diamond in Figure 4).

2. Figures and additional descriptions

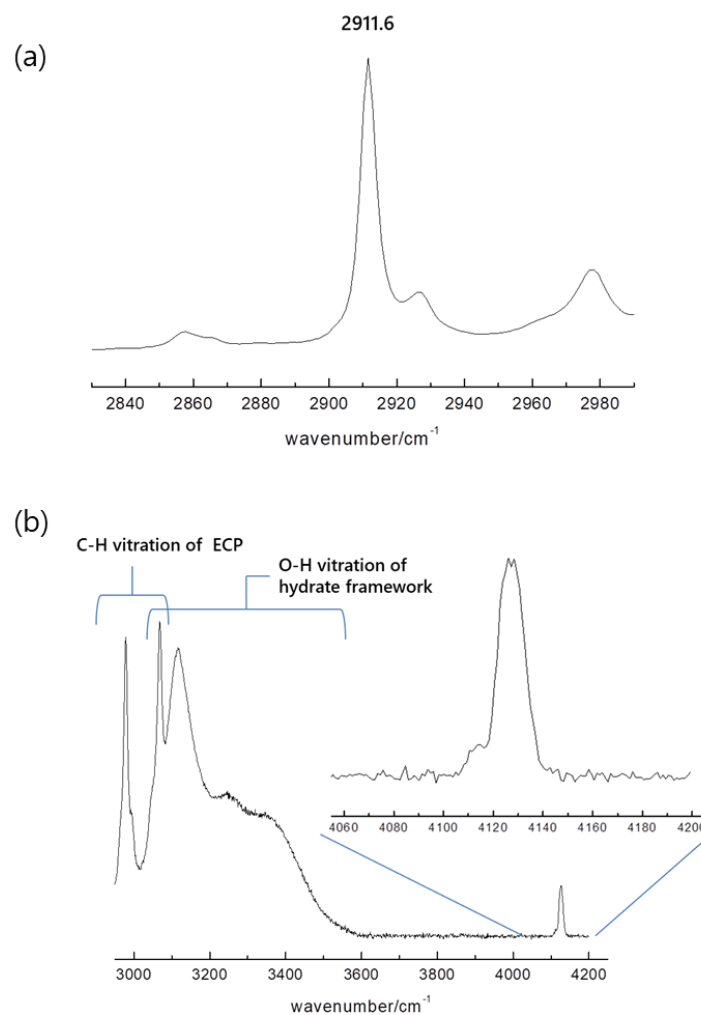


Figure S1. Raman spectra of (a) the ECP + CH₄ hydrate and (b) the ECP + H₂ hydrate measured at 123 K and at atmospheric pressure. (a) The peak at 2911.6 cm⁻¹ clearly indicates that CH₄ molecules are accommodated in sII-S cages. The other peaks near 2855, 2925, and 2975 cm⁻¹ are attributed to some C-H vibrations of the ECP molecule. (b) Typical peaks of H₂ molecules in sII-S cages were detected at 4110~4130 cm⁻¹ [4, 5, 16]. The two peaks near 4115 and 4127 cm⁻¹ are attributed to the ortho-para transition of the H₂ molecule [20, 21].

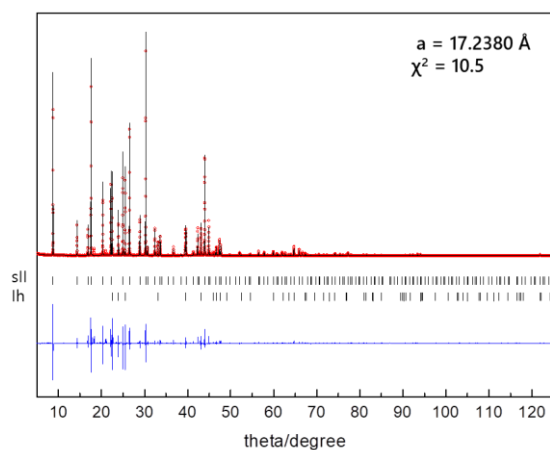


Figure S2. HRPD patterns of the ECP + H₂O hydrate measured at 150 K. The lattice parameters are in the order of ECP + CH₄ hydrate (17.2558 Å) > ECP + H₂O hydrate (17.2380 Å) \approx ECP + H₂ hydrate (17.2360 Å). The gas-free ECP hydrate appears to expand slightly when additional CH₄ molecules are accommodated in it. However, considering that the molecular size of H₂ is much smaller than that of CH₄, for the H₂ hydrate, it does not appear that any lattice expansion induced by H₂ enclathration occurred.

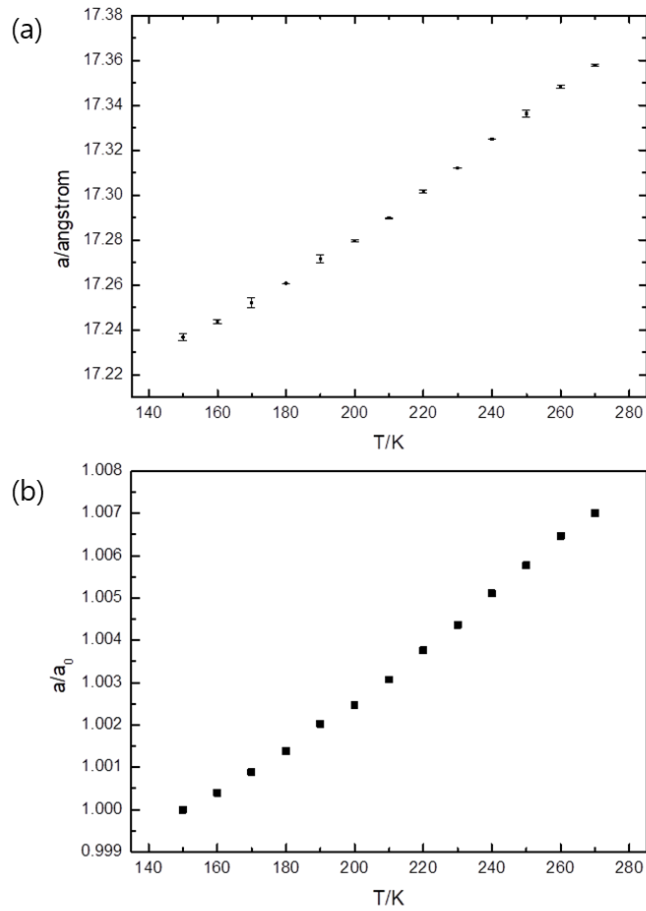


Figure S3. For the ECP + H₂O hydrate, (a) lattice parameters vs. temperature and (b) normalized lattice parameters vs. temperature (the lattice parameter at 150 K was set to a_0). The sII lattice expanded gradually with a nearly constant linear expansion coefficient of 5.8×10^{-5} , in good agreement with outcomes reported in several studies [12, 22-24]. Finally, the lattice parameter at 270 K becomes approximately 0.7% larger than that at 150 K. However, the clear patterns representing the sII structure collapsed when the sample was heated to 280 K. Therefore, we can conclude that the solid ECP hydrate dissociates at a certain temperature below 280 K.

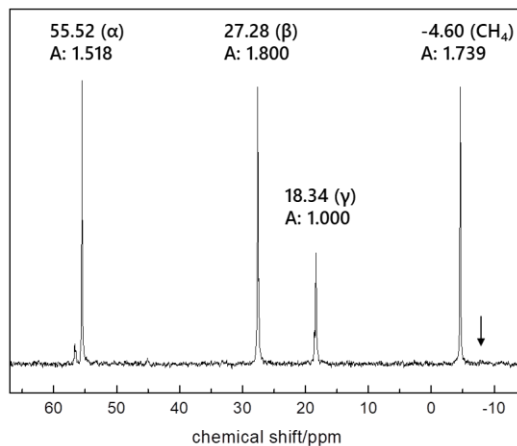


Figure S4. Full-range ^{13}C NMR spectrum of the ECP + CH_4 hydrate measured at 210 K. No signal was detected at -8.3 ppm (black arrow) due to the CH_4 in the sII-L cage (see Figure 3(a)).

In addition to the CH_4 peak at -4.60 ppm, three main peaks due to the ECP molecules were detected. From downfield to upfield, the peaks at +55.52, +27.28, and +18.34 ppm correspond to the α , β , and γ carbons of an ECP molecule, respectively. The actual area ratio was measured and found to be approximately 1.5:1.8:1.0, diverging somewhat from the ideal ratio of 2:2:1 expected on the basis of the number of each type of carbon. Many researchers [3, 7, 18, 25] have already demonstrated the methods by which to obtain the cage occupancy and to determine the composition of a hydrate by integrating the areas of the ^{13}C NMR peaks of different guests. However, we reported in a very recent study [26] that the functional group can affect the adjacent carbons (especially the α carbon) in some unexplained manner, leading to a slight reduction of the NMR intensity level. Thus, we used the peak of the γ carbon in this study, which is the carbon farthest from the oxygen atom, to obtain the molar ratio between ECP and CH_4 . Assuming that the large cages are fully occupied with ECP or CH_4 ($\theta_L = \theta_{L,ECP} + \theta_{L,CH_4} \approx 1$), the occupancy rate of CH_4 in the sII-S cages can be

calculated according to the following relationship.

$$\theta_{s,CH_4} = \frac{A_{s,CH_4}/2}{A_{L,ECP}/N_{EC} + A_{L,CH_4}}$$

Here, A is the relative area of each type of carbon and N_{EC} is the number of equivalent carbons. According to the values of the relative areas, we can find that $\theta_{s,CH_4} = 0.87$, a considerably higher value than those from other CH_4 hydrates. For example, Seo et al. [3] reported that the CH_4 occupancy rate of the THF + CH_4 hydrate is 0.37 at a stoichiometric concentration of THF. A more recent study reported that methane uptake in THF hydrate was approximately 0.07 mol CH_4 / mol H_2O [6], indicating a CH_4 occupancy rate of 0.60. For the CP + CH_4 hydrate, Lv et al. [27] reported θ_{s,CH_4} values in the range of 0.2 ~ 0.4, whereas Lee et al. [7] suggested a much higher value of 0.60 (see Table S3).

Figure 3(b): additional discription

In Figure 3(b), we can classify the peaks into the three groups of (1) a moderately broad peak centered at 4.1 ppm, (2) four sharp peaks in the range of 3.5~1.0 ppm, and (3) the broadest background peak centered at around 2 ppm. (1) The first peak is attributed to the H₂ molecules entrapped in the sII-S cages, highly consistent with earlier studies [4, 19]. (2) When we simply consider the Lewis structure, there are only three different types of hydrogen atoms in an ECP molecule with a corresponding number ratio of 2:4:2, leading to three peaks with the same area ratio. However, the somewhat complicated patterns observed in the second set of four peaks may have arisen due to combinations of the peaks from several conformers or enantiomers of ECP. (3) Thus, the remaining third peak may have arisen from the water framework. Several uncertain points remain, though it is clear that H₂ molecules are entrapped in sII-S cages. Here, the H₂ capacity was determined by the same method that reported by Strobel et al. [19]. The relative areas between the peak (1) and the set of four peaks (2) were approximately 1:3, indicative the H₂ occupancy of nearly 0.67. However, H₂ molecules exist in the form of ortho- and para- isomers, of which only the former is observable by ¹H NMR. Accordingly, given that the ratio of ortho-H₂ to para-H₂ is approximately 3 above 200 K, the actual H₂ occupancy becomes nearly 0.9. We assumed $\theta_{L,ECP} \approx 1$ and single H₂ occupancy of the small cage.

We additionally crosschecked the capacity from another way. The stoichiometric mixture of ECP + H₂O was quenched by liquid nitrogen in the form of thin film (t~0.2 mm). The solid sample was ground into a fine powder (d~120 μm), followed by pressurizing with ~100 bar of H₂ at 243 K. After 4 days, the volume of stored H₂ was directly measured by melting the sample. We found that average 93 cm³ of H₂ (STP) was stored in 1 g of the ECP + H₂ hydrate samples, indicative of 13 H₂ · 8 ECP · 136 H₂O and the $\theta_{S,H2} \approx 0.81$.

3. Tables

Table S1. Equilibrium P-T conditions of CH₄ hydrates containing promoters ($x_{\text{promoter}} = 0.0556$)

ECP		CP [7]		THF [15]		THF (this work)	
T (K)	P (bar)	T (K)	P (bar)	T (K)	P (bar)	T (K)	P (bar)
297.0	22.1	294.3	21.6	293.1	21.2	296.0	31.7
301.4	43.1	297.3	35.7	297.0	37.3	299.6	54.1
303.1	57.2	299.6	51.2	300.1	60.2	301.8	78.1
303.8	64.6	301.7	67.0	302.3	81.3		
305.8	83.7	303.0	86.1				

Table S2. Equilibrium P-T conditions for H₂ hydrates containing promoters ($x_{\text{promoter}} = 0.0556$)

ECP		CP [2]		THF [16]	
T (K)	P (bar)	T (K)	P (bar)	T (K)	P (bar)
282.5	26.6	280.7	27.0	278.2	21.3
283.6	48.3	281.6	49.4	279.2	48.7
284.3	68.2	282.4	70.0	280.1	83.0
284.9	84.0	283.1	90.4	280.8	113
285.5	107.5	283.7	111		

Table S3. CH₄ occupancies, compositions, and CH₄ contents of THF, CP, or ECP + CH₄ hydrate

	ECP + CH ₄	THF + CH ₄	THF + CH ₄	CP + CH ₄	CP + CH ₄
θ_{S,CH_4}	0.87	0.37 [3]	0.60	0.30 [43]	0.60 [7]
x CH ₄ · 8 LGM · 136 H ₂ O ^a	13.9	5.9	9.5	4.8	9.6
mmol CH ₄ / mol H ₂ O	102	43	70 [6]	35	71

^a LMG: large guest molecules

Table S4. Physical properties and safety data of THF, CP, and ECP^a

	P ^{sat} (kPa) ^b	T _b (°C)	T _f (°C)	ρ (g/ml) ^b	Hazard statements
THF	19.3	66	-21	0.880	H225, H302, H319, H335, H336, H351
CP	36	50	-7 (-20 ^c)	0.745	H225, H304, H315 ^c , H319 ^c , H335 ^c , H336, H412
ECP	6.0 ^d	102	10	0.964	H225, H315, H319, H335

^a from [28].

^b values at 293 K.

^c additional data from [29].

^d see reference [30].

4. References

* References 1~19: see main text

[20] K. Shin, Y. Kim, T. A. Strobel, P. S. R. Prasad, T. Sugahara, H. Lee, E. D. Sloan, A. K. Sum, and C. A. Koh, *J. Phys. Chem. A* 2009, **113**, 6415.

[21] M. Cha, M. Kwon, Y. Youn, K. Shin, and H. Lee, *J. Chem. Eng. Data* 2012, **57**, 1128.

[22] K. C. Hester, Z. Huo, A. L. Ballard, C. A. Koh, K. T. Miller, and E. D. Sloan, *J. Phys. Chem. B* 2007, **111**, 8830.

[23] Y. Park, Y. N. Choi, S. -H. Yeon, and H. Lee, *J. Phys. Chem. B* 2008, **112**, 6897.

[24] M. Cha, Y. Youn, M. Kwon, K. Shin, S. Lee, and H. Lee, *Chem. Asian J.* 2012, **7**, 122.

[25] Y. Seo and H. Lee, *J. Phys. Chem. B* 2002, **106**, 9668.

[26] J. Seol, Clathrate hydrate containing nitro compounds: Application to energy storage and transport, *10th International Conference on Gas Hydrates* 2020, accepted.

[27] Q. Lv and X. Li, *Energy Procedia*, 2017, 142, 3264-3269.

[28] Material Safety Data Sheets of Thermo Fisher Scientific Chemicals, Inc.

[29] Safety Data Sheet of Sigma-Aldrich, Inc.

[30] (a) A. E. Meshechkina, L. V. Mel'nik, G. V. Rybina, S. S. Srednev, Y. A. Moskvichev, A. S. Danilova, Z. V. Kostyuk, *Russian J. Appl. Chem.* 2009, **82**, 925. (b) The P^{sat} (at 293 K) value of ECP was calculated by the Clausius-Clapeyron equation using the data reported in (a).